may appear simultaneously with cognitive problems in patients with usual NPH.[37] A major dilemma therefore exists in patients with VS who commonly complain of balance disturbance. These disturbances are usually attributed to vestibular insufficiency or cerebellar symptoms. In fact, we could not decide whether shunt placement surgery was indicated for a patient who presented with mild ventricular dilation and a slightly unsteady gait or balance disturbance. Therefore in this series, the VP shunt placement operation was postponed in all patients until their gait disturbance and CSF space enlargement became obvious. Regis and colleagues[31] reported that approximately one quarter (26%) of patients who did not have a balance disturbance before treatment suffered from it after they underwent SRS. In previous reports, balance disturbance has been expressed as unsteadiness, dizziness, dysequilibrium, or imbalance; some of these symptoms may be caused by early-stage CSF malabsorption. It should be noted that mild gait unsteadiness or slight cognitive dysfunction with reduced daily activity may be the initial manifestation of CSF malabsorption.

The clinical presentation of common NPH may appear years after the development of enlarged ventricles and is always progressive, albeit variable in terms of rate.[37] In the present series, placement of a shunt was required to resolve progressive clinical symptoms 4 to 20 months after fractionated SRT, with a median of 12 months. This is somewhat different from the usual course of NPH. In this period following fractionated SRT, irradiated VS tissue may cause degenerative changes, as shown in Fig. 3. The tumor, including necrotic debris, may release some large molecules into the CSF, which could aggravate preexisting CSF malabsorption to a level that produces symptoms. The spontaneous resolution of the ventricular enlargement, shown in Fig. 5, may further support this speculation. The amounts of protein in the CSF of our patients with ventricular dilation, however, remained within the normal range (data not shown). A special laboratory investigation will be required to validate our assumption.

Thomsen, et al.,[40] observed a patient with symptomatic hydrocephalus that developed after GKS and suggested the importance of careful observation of such patients. Communicating hydrocephalus is an important complication, but probably not an adverse effect specific to SRT for VS. A previous report from Sweden on GKS showed a 10% incidence of shunt operations in 312 patients and a 4% incidence of new hydrocephalus after SRS.[23] In the series conducted by Regis and colleagues[31] three (3%) of 97 patients required a shunt. Hydrocephalus requiring shunt placement was also reported in 3% of patients by Kondziolka, et al.,[11] and in three (5%) of 56 patients reported on by Mendenhall and coworkers.[18] In our series, 11 (11%) of 101 patients required a shunt although there was no evidence of tumor growth. The size (25.5 mm) of the 11 tumors that caused symptomatic communicating hydrocephalus was significantly larger than that (18.2 mm) of the tumors that did not. The present study included relatively large VSs, with maximum diameters as large as 40 mm. If large tumors (> 25 mm in maximum diameter) are excluded, only four (5.5%) of 72 patients required a shunt for symptomatic communicating hydrocephalus. This is not a surprising difference from the results of SRS series. The only exception is reported by Prasad and associates,[30] who observed no posttreatment hydrocephalus in 153 patients treated by GKS during a follow-up period that lasted longer than 4 years. They treated tumors ranging in volume from 0.02 to 18.3 cm^3 (mean 2.8 cm^3) including 19 large lesions whose sizes were greater than 30 × 20 × 20 mm (volumes > 6.5 cm^3). We cannot explain these observations, which are quite dissimilar from ours and the aforementioned results of Pirouzmand, et al.,[25] who found that 36 of 284 patients had ventricular dilation consistent with NPH. Certain differences may exist in the follow-up protocol, method of treatment, and/or size of tumors treated. Although Prasad and associates obtained precise documentation from both patients and referring physicians, only a small number of patients returned to their institution for office visits. In contrast, two thirds of our patients, particularly those harboring a large VS, returned to our institution for regular follow-up visits to receive neurological examination and MR imaging, including imaging of whole ventricles. Alternatively, fractionated radiotherapy may be more effective to destroy the tumor cells and produce degenerative debris than radiosurgery. Last, the smaller size of tumors in the series conducted by Prasad and associates is the most probable reason for the difference. These hypotheses cannot be ruled out by the retrospective analysis and should be investigated further.

Considering the excellent tumor control and functional preservation attained after fractionated SRT, the requirement of a shunt placement operation in a small proportion of patients may not constitute a stumbling block for fractionated SRT or SRS. Alternatively, based on the present study we recommend careful long-term neurological observation for at least several years after radiotherapy, especially when large VSs have been treated. The interval between follow-up examinations in this study (every 6 months) appeared to be reasonable, considering the good outcomes observed after shunt placement.

Conclusions

Fractionated stereotactic radiotherapy produced an adequate tumor-control rate, even for relatively large tumors, and an excellent rate of hearing preservation that was comparable to the best results published for single-fraction radiosurgery. Because a small number of patients required neurosurgical treatment long after fractionated SRT, a careful long-term follow-up review is necessary, particularly to monitor patients for communicating hydrocephalus. This may also be true for radiosurgery.

References

1. Atlas MD, Perez de Tagle JR, Cook JA, et al: Evolution of the management of hydrocephalus associated with acoustic neuroma. **Laryngoscope 106:**204–206, 1996
2. Battista RA, Wiet RJ: Stereotactic radiosurgery for acoustic neuromas: a survey of the American Neurootology Society. **Am J Otol 21:**371–381, 2000
3. Briggs RJ, Shelton C, Kwartler JA, et al: Management of hydrocephalus resulting from acoustic neuromas. **Otolaryngol Head Neck Surg 109:**1020–1024, 1993
4. Committee on Hearing and Equilibrium: Committee on Hearing and Equilibrium guidelines for the evaluation of hearing preservation in acoustic neuroma (vestibular schwannoma). **Otolaryngol Head Neck Surg 113:**179–180, 1995
5. Flickinger JC, Kondziolka D, Niranjan A, et al: Results of acoustic

neuroma radiosurgery: an analysis of 5 years'experience using current methods. **J Neurosurg 94:**1–6, 2001
6. Foote KD, Friedman WA, Buatti JM, et al: Analysis of risk factors associated with radiosurgery for vestibular schwannoma. **J Neurosurg 95:**440–449, 2001
7. Fuss M, Debus J, Lohr F, et al: Conventionally fractionated stereotactic radiotherapy (FSRT) for acoustic neuromas. **Int J Radiat Oncol Biol Phys 48:**1381–1387, 2000
8. Gardner G, Robertson JH: Hearing preservation in unilateral acoustic neuroma surgery. **Ann Otol Rhinol Laryngol 97:**55–66, 1988
9. House JW, Brackmann DE: Facial nerve grading system. **Otolaryngol Head Neck Surg 93:**146–147, 1985
10. Kagei K, Shirato H, Suzuki K, et al: Small-field fractionated radiotherapy with or without stereotactic boost for vestibular schwannoma. **Radiother Oncol 50:**341–347, 1999
11. Kondziolka D, Lunsford LD, McLaughlin MR, et al: Long-term outcomes after radiosurgery for acoustic neuromas. **N Engl J Med 339:**1426–1433, 1998
12. Koos WT, Day JD, Matula C, et al: Neurotopographic considerations in the microsurgical treatment of small acoustic neurinomas. **J Neurosurg 88:**506–512, 1998
13. Lederman G, Arbit E, Lowry J: Management of acoustic neuroma. **N Engl J Med 340:**1119–1120, 1999 (Letter)
14. Lederman G, Lowry J, Wertheim S, et al: Acoustic neuroma: potential benefits of fractionated stereotactic radiosurgery. **Stereotact Funct Neurosurg 69:**175–182, 1997
15. Maire JP, Caudry M, Darrouzet V, et al: Fractionated radiation therapy in the treatment of stage III and IV cerebello-pontine angle neurinomas: long-term results in 24 cases. **Int J Radiat Oncol Biol Phys 32:**1137–1143, 1995
16. Malis L: Gamma surgery for vestibular schwannoma. **J Neurosurg 92:**894–896, 2000
17. Meijer OW, Wolbers JG, Baayen JC, et al: Fractionated stereotactic radiation therapy and single high-dose radiosurgery for acoustic neuroma: early results of a prospective clinical study. **Int J Radiat Oncol Biol Phys 46:**45–49, 2000
18. Mendenhall WM, Friedman WA, Buatti JM, et al: Preliminary results of linear accelerator radiosurgery for acoustic schwannomas. **J Neurosurg 85:**1013–1019, 1996
19. Miller RC, Foote RL, Coffey RJ, et al: Decrease in cranial nerve complications after radiosurgery for acoustic neuromas: a prospective study of dose and volume. **Int J Radiat Oncol Biol Phys 43:**305–311, 1999
20. Moller P, Myrseth E, Pedersen PH, et al: Acoustic neuroma—treatment modalities. Surgery, gamma-knife or observation? **Acta Otolaryngol Suppl 543:**34–37, 2000
21. Nakamura H, Jokura H, Takahashi K, et al: Serial follow-up MR imaging after gamma knife radiosurgery for vestibular schwannoma. **AJNR 21:**1540–1546, 2000
22. Niranjan A, Lunsford LD, Flickinger JC, et al: Dose reduction improves hearing preservation rates after intracanalicular acoustic tumor radiosurgery. **Neurosurgery 45:**753–765, 1999
23. Norén G, Greitz D, Hirsh A, et al: Gamma knife radiosurgery in acoustic neurinomas, in Tos M, Thomsen J (eds): **Acoustic Neuroma.** Amsterdam: Kugler Publications, 1992, pp 289–292
24. Pendl G, Ganz JC, Kitz K, et al: Acoustic neurinomas with macrocysts treated with gamma knife radiosurgery. **Stereotact Funct Neurosurg 66 (Suppl 1):**103–111, 1996
25. Pirouzmand F, Tator CH, Rutka L: Management of hydrocephalus associated with vestibular schwannoma and other cerebellopontine angle tumors. **Neurosurgery 48:**1246–1254, 2001
26. Poen JC, Golby AJ, Forster KM, et al: Fractionated stereotactic radiosurgery and preservation of hearing in patients with vestibular schwannoma: a preliminary report. **Neurosurgery 45:** 1299–1307, 1999
27. Pollock BE, Lunsford LD, Flickinger JC, et al: Vestibular schwannoma management. Part I. Failed microsurgery and the role of delayed stereotactic radiosurgery. **J Neurosurg 89:**944–948, 1998
28. Pollock BE, Lunsford LD, Kondziolka D, et al: Vestibular schwannoma management. Part II. Failed radiosurgery and the role of delayed microsurgery. **J Neurosurg 89:**949–955, 1998
29. Prasad D: Vestibular schwannomas: radiosurgery. **J Neurosurg 94:**141–142, 2001 (Letter)
30. Prasad D, Steiner M, Steiner L: Gamma surgery for vestibular schwannoma. **J Neurosurg 92:**745–759, 2000
31. Regis J, Pellet W, Delsanti C, et al: Functional outcome after gamma knife surgery or microsurgery for vestibular schwannomas. **J Neurosurg 97:**1091–1100, 2002
32. Sakamoto T, Shirato H, Sato N, et al: Audiological assessment before and after fractionated stereotactic irradiation for vestibular schwannoma. **Radiother Oncol 49:**185–190, 1998
33. Sakamoto T, Shirato H, Takeichi N, et al: Medication for hearing loss after fractionated stereotactic radiotherapy (SRT) for vestibular schwannoma. **Int J Radiation Oncol Biol Phys 50:** 1295–1298, 2001
34. Samii M, Matthies C: Gamma surgery for vestibular schwannoma. **J Neurosurg 92:**892–896, 2000
35. Shirato H, Sakamoto T, Sawamura Y, et al: Comparison between observation policy and fractionated stereotactic radiotherapy (SRT) as an initial management for vestibular schwannoma. **Int J Radiat Oncol Biol Phys 44:**545–550, 1999
36. Shirato H, Sakamoto T, Takeichi N, et al: Fractionated stereotactic radiotherapy for vestibular schwannoma (VS): comparison between cystic-type and solid-type VS. **Int J Radiat Oncol Biol Phys 48:**1395–1401, 2000
37. Snow RB: Neurosurgical aspects of dementia, in Tindall GT, Cooper PR, Barrow DL (eds): **The Practice of Neurosurgery.** Baltimore: Williams & Wilkins, 1996, Vol 1, pp 215–222
38. Spiegelmann R, Lidar Z, Gofman J, et al: Linear accelerator radiosurgery for vestibular schwannoma. **J Neurosurg 94:**7–13, 2001
39. Suh JH, Barnett GH, Sohn JW, et al: Results of linear accelerator-based stereotactic radiosurgery for recurrent and newly diagnosed acoustic neuromas. **Int J Cancer 90:**145–151, 2000
40. Thomsen J, Tos M, Bøgesen SE: Hydrocephalus caused by gamma knife treatment of an acoustic neuroma. in Tos M, Thomsen J (eds): **Acoustic Neuroma.** Amsterdam: Kugler Publications, 1992, pp 311–314
41. Unger F, Walch C, Haselsberger K, et al: Radiosurgery of vestibular schwannomas: a minimally invasive alternative to microsurgery. **Acta Neurochir 141:**1281–1286, 1999
42. Urich H, Tien RD: Tumors of the cranial, spinal and pripheral nerve sheaths, in Bigner DD, McLendon RE, Bruner JM (eds): **Russell and Rubinstein's Pathology of Tumors of the Nervous System, ed 6.** London: Arnold, 1998, pp 141–194
43. Varlotto JM, Shrieve DC, Alexander E III, et al: Fractionated stereotactic radiotherapy for the treatment of acoustic neuromas: preliminary results. **Int J Radiat Oncol Biol Phys 36:**141–145, 1996
44. Wallner KE, Sheline GE, Pitts LH, et al: Efficacy of irradiation for incompletely excised acoustic neurilemomas. **J Neurosurg 67:** 858–863, 1987

Manuscript received January 21, 2003.
Accepted in final form June 5, 2003.
Address reprint requests to: Yutaka Sawamura, M.D., Ph.D., Department of Neurosurgery, Hokkaido University School of Medicine, North-15, West-7, Kita-ku, Sapporo 060, Japan. email: ysawamu@med.hokudai.ac.jp.

ELSEVIER

Int. J. Radiation Oncology Biol. Phys., Vol. 60, No. 1, pp. 214–217, 2004

0360-3016/04/$ - see front matter

doi:10.1016/j.ijrobp.2004.02.024

CLINICAL INVESTIGATION **Brain**

IMPACT OF MARGIN FOR TARGET VOLUME IN LOW-DOSE INVOLVED FIELD RADIOTHERAPY AFTER INDUCTION CHEMOTHERAPY FOR INTRACRANIAL GERMINOMA

HIROKI SHIRATO, M.D., HIDEFUMI AOYAMA, M.D., JUN IKEDA, M.D., KENJI FUJIEDA, M.D., NORIO KATO, M.D., NOBUAKI ISHII, M.D., KAZUO MIYASAKA, M.D., YOSHINOBU IWASAKI, M.D., AND YUTAKA SAWAMURA, M.D.

Departments of Radiology, Neurosurgery, and Pediatrics, Hokkaido University School of Medicine, Sapporo, Japan

Purpose: We previously published a report stating that germinomas with elevated serum beta human chorionic gonadotropin (HCG-β) had a poor relapse rate, but these findings have not been supported by a multi-institutional trial. The margin for initial gross tumor volume (GTV) before surgery and chemotherapy of the same materials was investigated by retrospective review.

Methods and Material: The 27 patients reported on in the previous paper were analyzed. The two-dimensional margin from the initial GTV to 90% of the prescribed dose of 24 Gy was 2.0 cm for a solitary lesion in the protocol. This margin was measured retrospectively without knowledge of the serum HCG-β level. The whole ventricle field was used for patients with multifocal disease and whole central nervous system field was used for disseminated disease, respectively.

Results: Six relapses were seen in 18 patients with solitary tumors, and were treated with the minimum margin of 1.5 cm or less to the initial GTV. Five of the 6 had initially elevated serum HCG-β at the median of 7.4 mIU/mL, ranging from 0.7–233 mIU/mL. No relapses were seen in the 9 patients who were treated with whole ventricle or whole central nervous system field.

Conclusions: An inadequate margin and elevated serum HCG-β were equally determined to be candidates that caused the poor local control. The whole ventricle is recommended as the smallest target volume for germinoma with or without elevated HCG-β after induction chemotherapy. © 2004 Elsevier Inc.

Germinoma, Central nervous system, Radiotherapy, Induction chemotherapy.

INTRODUCTION

Whole ventricle or larger fields have been the standard of care for intracranial germinoma in our institution (1), as in other institutions (2–4). The possibility of reducing the dose and volume was suggested by the usage of cisplatin-based chemotherapy in the early 1990s (5). A Phase II study on induction cisplatin-based chemotherapy for germinomas followed by 24 Gy radiotherapy was conducted as a regional study in the Hokkaido district of Japan (6). The results of the Phase II study showed a higher relapse rate in germinomas with elevated serum human chorionic gonadotropin beta (HCG-β) than in those without elevated serum HCG-β (7). However, a nationwide prospective study using platinum-based induction chemotherapy followed by low-dose radiotherapy for 130 germinoma patients without elevation of HCG-β, and 34 germinoma patients with elevated HCG-β, did not show significant differences in the relapse-free rate between germinomas without elevated serum HCG-β and germinomas with elevated serum HCG-β (8). Furthermore, treatment volume was reported to be a significant prognostic factor in the nation-wide study. This discrepancy in the significance of HCG-β and the treatment volume prompted us to reevaluate the treatment results of the Hokkaido study by conducting a precise review of the treatment volume.

The purpose of this study is to investigate the impact of margins for the target volume in low-dose involved field radiotherapy after induction chemotherapy for intracranial germinoma.

METHODS AND MATERIALS

The eligibility criteria for patients receiving the induction chemotherapy followed by low-dose radiotehrapy were (*1*) 3 years old or older, (*2*) histologically proven germinoma, and (*3*) no previous chemotherapy or radiotherapy. The patients were classified into two groups as follows: (*1*) a good prognosis group, consisting of patients with a solitary

Reprint requests to: Hiroki Shirato, M.D., Department of Radiology, Hokkaido University School of Medicine, North-15 West-7, Kita-ku, Sapporo 060-8638, Japan. Tel: (+81) 11-706-5975; Fax: (+81) 11-706-7876; E-mail: hshirato@radi.med.hokudai.ac.jp

Received Oct 17, 2003, and in revised form Feb 6, 2004. Accepted for publication Feb 9, 2004.

germinoma with serum HCG-β < 0.5 mIU/mL, which was the normal upper limit in our institute, and (*2*) an intermediate prognosis group, consisting of patients with a solitary germinoma with HCG-β ≥ 0.5 mIU/mL, a multifocal germinoma (two or more lesions without evidence of dissemination), and disseminated germinoma (cytological or imaging evidence of dissemination). For the good prognosis group, 3–4 cycles of etoposide (100 mg/m^2) and cisplatin (20 mg/m^2) were given for 5 days every 4 weeks. For the intermediate prognosis group, 3–6 cycles of ifosfamide (900 mg/m^2), cisplatin (20 mg/m^2), and etoposide (60 mg/m^2) were given for 5 days every 4 weeks. After the induction chemotherapy, 24 Gy in 12 fractions in 3 weeks were given to the clinical target volume (CTV) as follows: for solitary germinomas, involved fields, or the initial gross tumor volume (GTV) with a two-dimensional (2D) margin of 2 cm; for multifocal germinoma, whole ventricles; and for disseminated germinoma, whole central nervous system (CNS). The CTV was not altered by the level of serum HCG-β. Within 2 weeks after the completion of the last course of chemotherapy, radiotherapy was started based on computed tomographic (CT) planning with slice-by-slice determination of the target volume. Magnetic resonance imaging (MRI) was used only as the reference, and no image fusion technique was used in the planning. No boost irradiation was used after the 24 Gy irradiation. First salvage treatment for the relapse was predetermined in the protocol as the same chemotherapy followed by whole brain or whole CNS irradiation of 24 Gy. Consequently, the maximum cumulative dose is then 48 Gy to the initial PTV and 24 Gy to the whole brain or whole CNS, respectively, if tumors relapse in patients who have already been treated with focal volume as the initial treatment. Six or 10 MV X-rays were used with multiple portals for the involved fields, parallel opposed fields for the whole ventricles and whole brain, and posterior tandem fields for the whole spinal irradiation, respectively.

Treatment planning was performed with Therac (NEC, Tokyo, Japan) from 1992–1995, and with Focus (CMS Japan, Tokyo, Japan) after 1995. Three-dimensional dose distribution was available for the transaxial, coronal, and sagittal views at the isocenter for patients who were treated with involved fields or whole ventricle fields. The concept of planning target volume (PTV) and CTV was not well understood at the start of this study, and CTV was covered by the isodose curve of 90% of the dose prescribed at the isocenter. In the present study, all CT and MRI slices before surgery/chemotherapy and those for radiotherapy planning were retrospectively reviewed for all the patients entered in the study. A radiation oncologist (H.A.) surveyed the 2D minimum distance between the tumor size before surgery/induction chemotherapy and the 90% isodose surface. The retrospective review was based on the careful visual correlation between planning-based CT and the diagnostic CT or MRI studies but not on image fusion techniques. The serum HCG-β was blinded to the investigator at the time of analysis. For the comparison between two categories, the chi-square test was used. Kaplan-Meier analysis and the log-rank test were used for the survival analysis.

Table 1. Information on the 6 patients who experienced tumor relapse

	Serum HCG-β (mIU/mL)	TV	Site of failure relative to TV	Spinal relapse
Elevated				
1	101	Local	Outside	
2	233	Local	Margin	
3	0.7	Local	Outside	Yes
4	5.3	Local	Outside	
5	0.7	Local	In and outside	
Nonelevated				
6	<0.5	Local	Outside	Yes

Abbreviations: HCG = human chorionic gonadotropin; TV = treated volume.

RESULTS

Between February 1992 and November 1999, 27 patients were entered in the study, as reported in the previous article (7). Age was 15.7 years old at median, distributed from 8–28 years. Twenty patients were 18 years old or younger and 7 patients were more than 18 years old. Cytology of craniospinal fluid, enhanced cranial MRI, and enhanced spinal MRI were used in staging work-up in all patients. The follow-up period was 58 months at median, ranging from 18–102 months. All but 1 patient was followed more than 24 months. Sixteen patients showed a normal serum HCG-β level, which was < 0.5 mIU/mL in our institution, and 11 patients showed elevated HCG-β with the mean at 7.4 mIU/mL, and the range from 0.7–233 mIU/mL. Serum HCG-β was elevated in 8 of the 18 patients with solitary tumors, 2 of the 6 patients with multifocal tumors, and 1 of the 3 patients with disseminated tumors. These were all treated with 24 Gy in 12 fractions in 3 weeks for the involved fields, whole ventricle, and whole CNS irradiation, respectively.

The disease-specific survival at 5 years was 100%, and the overall survival was 95%. The relapse-free survival at 5 years, according to the serum HCG-β level, was 90% for patients with normal HCG-β and 44% for patients with elevated serum HCG-β (p = 0.025). When we allowed for the first salvage treatment administered when relapse occurred, the tumor control rate was 95% at 5 years.

Details on the patients who experienced treatment failure are shown in Table 1. Five of 6 relapses were observed in patients with elevated serum HCG-β. All patients were treated with involved fields. The site of failure relative to the treated volume (TV), covered by 90% of the prescribed dose, was outside the TV in 4 (2 had spinal lesions), the marginal site in 1, and outside and in the TV (2 relapses) in 1 patient. Therefore, the local failure rate was 3.7% for the

Table 2. Relationship between the serum HCG-β, treated volume, and disease control in 27 patients with intracranial germinoma

Clinical subtype	Treated volume			
	Local	WV	WCNS	Total
Total	12/18	6/6	3/3	21/27
Serum HCG-β <0.5 mIU/mL	9/10	4/4	2/2	15/16
Serum HCG-β elevated	3/8	2/2	1/1	6/11

Abbreviations: HCG = human chorionic gonadotropin; WV = whole ventricle; WCNS = whole central nervous system.

definite in-field relapse, and 7.4% for the marginal or in-field relapse.

Table 2 shows the relationship between the serum HCG-β, treated volume, and relapse ratio. There were no relapses in 9 patients who were treated for whole ventricle or whole CNS. A small treatment volume and elevated serum HCG-β were equally considered candidates for causing the poor local control.

Even though the 2D margin for the initial GTV was determined to be 2.0 cm or more in the protocol, 12 of 27 patients were treated with < 2.0 cm, and 10 with < 1.5 cm margin. Most tumors were very small or not visible in the planning CT and MRI at the time of radiotherapy, because of the efficacy of the induction chemotherapy. All 6 relapses were treated with a 2D margin <1.5 cm. There were no relapses in 4 patients who had elevated serum HCG-β and who were treated with whole ventricle or larger fields. The whole ventricle field included the fourth ventricle. There was a statistically significant difference in the relapse ratio between patients treated with a 2D margin < 1.5 cm (median, 1.0 cm; range, 0.5–1.2 cm), and those with a 2D margin ≥ 1.5 cm (median, 2.4 cm; range, 1.5–2.8 cm; $p < 0.01$; Table 3).

The complications due to treatment were azoospermina in 1 of 4 patients examined. One patient experienced anterior pituitary hormonal replacement owing to relapse at the neurohypophyseal region. No new onset or deterioration in anterior pituitary function was noted. Three of 7 adult patients older than 18 years at the time of treatment married after treatment, and 1 fathered a child.

Table 3. Relationship between serum HCG-β, 2D margin, and relapse ratio in 27 patients with intracranial germinoma

Serum HCG-β	*2D margin* <1.5 cm	*2D margin* >1.5 cm
<0.5 mIU/mg	1/3	0/13
>0.5 mIU/mg	5/7	0/4

Abbreviations: HCG = human chorionic gonadotropin; 2D = two-dimensional.

DISCUSSION

It is well known that localized treated volume results in a high relapse rate in intracranial germinoma. In a multi-institutional retrospective survey, Aoyama *et al.* (9) showed that the 5-year relapse-free rate was significantly lower in patients treated with localized volume than whole ventricle or larger volume. Because a high incidence of radiation-related late complications have been noted after large volume irradiation for pediatric patients, induction chemotherapy has been expected to reduce the amount of radiation volume and dose. There are pros and cons to this opinion (3–5, 10–14). The possible incidence of relapses using lower doses and smaller volumes is the shortcoming of this approach to this highly curable disease. Pretreatment impairment in neurocognitive function due to the tumor or surgery is also suggested to be a possible bias in the opinion against radiotherapy (15, 16). The lack of well-controlled randomized trials and the small number of patients in each institution has forced us, at present, to conduct a careful analysis of the prospective Phase II studies to speculate on the best treatment method.

Elevated serum HCG-β was reported to be a poor prognostic factor for patients with intracranial germinoma treated with chemotherapy alone in a large multi-institutional study (11). We have analyzed our data to evaluate the prognostic importance of serum HCG-β based on the previous report, and found the possible importance of serum HCG-β in our series (7). A Japanese multi-institutional cooperative group began to treat intracranial germinoma with platinum-based induction chemotherapy followed by 24 Gy irradiation 6 years ago, and treated more than 100 patients. Preliminary reports of the large Phase II study suggested that HCG-β was not a prognostic factor, and that a smaller treatment volume was associated with a higher relapse rate (8).

The small number of patients in our study prevented us from determining whether elevated serum HCG-β or an inadequate CTV margin was the predominant prognostic factor. The patients with relapsed tumors were treated with a small margin, and also had a higher serum HCG-β. Notably, there were no relapses in patients who were treated with whole ventricle or a larger volume, despite the fact that these patients had a larger tumor burden than those who were treated with involved fields. The tumor mass before chemotherapy was often massive or infiltrative, but the tumor was very small or not visible at the time of treatment planning. These differences in size and the anatomic shift of the normal brain made it difficult to determine the appropriate CTV based on the initial GTV before surgery and chemotherapy. Image fusion between the initial MRI and treatment planning CT after chemotherapy would be difficult, because of the anatomic shift of the normal brain tissues. The high incidence of violation in using 2.0 cm margins for the initial GTV may be partly due to these limitations in modern diagnostic imaging techniques rather than inadequate skills on the part of the treating physicians.

Interobserver variation must be large, even when utilizing the advanced imaging technologies available at present. Therefore, it is still difficult to achieve good quality assurance and a good quality control program for using the involved field for intracranial germinoma in a multi-institutional study.

Considering the low relapse rate in the treated volume in this study, 3.7% 7.4%, induction chemotherapy may reduce the dose required for the eradication of gross tumors. We did not use any boost dose in this study or in the Japanese multi-institutional study. Recent studies in western countries show that physicians are still using a boost dose to the tumor bed, giving 40–50 Gy in total (10, 11). Our results suggest that a prospective multi-institutional study is needed to test whether a boost dose to the tumor bed is necessary. Elimination or reduction in the boost dose after 24 Gy has a high probability of reducing vascular complications and deterioration in the anterior pituitary function. It is necessary to carefully monitor the long-term adverse effects of chemotherapy. Reduction of the radiation dose without chemotherapy would also be an important subject for a multi-institutional study.

In conclusion, the relapse rate can be unacceptably high in patients who were treated with involved fields, partly because of the difficulty in accurately determining the initial GTV before surgery and chemotherapy. Although the total tumor control rate after initial salvage treatment was high, it is obvious that tumor relapse should be avoided. In this respect, whole ventricle or larger field is still the target volume, which should be regarded as the standard both for germinoma with normal HCG-β, and for germinoma with elevated HCG-β, both in chemoradiotherapy and in radiotherapy alone.

REFERENCES

1. Shirato H. Nishio M. Sawamura Y. *et al.* Analysis of long-term treatment of intracranial germinoma. *Int J Radiat Oncol Biol Phys* 1997;37:511–515.
2. Shibamoto Y. Abe M. Yamashita J. *et al.* Treatment results of intracranial germinoma as a function of the irradiated volume. *Int J Radiat Oncol Biol Phys* 1988;15:285–290.
3. Wolden SK. Wara WM. Larson DA. *et al.* Radiation therapy for primary intracranial germ-cell tumors. *Int J Radiat Oncol Biol Phys* 1995;32:943–949.
4. Merchant TE. Sherwood SH. Mulhern RK. *et al.* CNS germinoma: Disease control and long-term functional outcome for 12 children treated with craniospinal irradiation. *Int J Radiat Oncol Biol Phys* 2000;46:1171–1176.
5. Allen JC. DaRosso RC. Donahue B. Nirenberg A. A phase II trial of preirradiation carboplatin in newly diagnosed germinoma of the central nervous system. *Cancer* 1994;74:940–944.
6. Sawamura Y. Shirato H. Ikeda J. *et al.* Induction chemotherapy followed by reduced-volume radiation therapy for newly diagnosed central nervous system germinoma. *J Neurosurg* 1998;88:66–72.
7. Aoyama H. Shirato H. Ikeda J. *et al.* Induction chemotherapy followed by low-dose involved field radiotherapy for intracranial germ cell tumors. *J Clin Oncol* 2002;20:857–865.
8. Matsutani M. for the Japanese Pediatric Brain Tumor Study Group. Combined chemotherapy and radiation therapy for CNS germ cell tumors—the Japanese experience. *J Neurooncol* 2001;54:311–316.
9. Aoyama H. Shirato H. Kakuto Y. *et al.* Pathologically-proven intracranial germinoma treated by radiation therapy. Radiother Oncol 1998;47:201–205.
10. Bamberg M. Kortmann RD. Calaminus G. *et al.* Radiation therapy for intracranial germinoma: Results of the German cooperative prospective trial MAIKEI 83/86/89. *J Clin Oncol* 1999;17:2585–2592.
11. Balmaceda C. Heller G. Rosenblum M. *et al.* Chemotherapy without irradiation—a novel approach for newly diagnosed CNS germ cell tumors: Results of an international cooperative trial. *J Clin Oncol* 1996;14:2908–2915.
12. Merchant TE. Davis BJ. Sheldon JM. *et al.* Radiation therapy for relapsed CNS germinoma after primary chemotherapy. *J Clin Oncol* 1998;16:204–209.
13. Lindstadt D. Wara WM. Edwards MSB. *et al.* Radiotherapy of primary intracranial germinoma: The case against routine craniospinal irradiation. *Int J Radiat Oncol Biol Phys* 1998;15:291–297.
14. Buckner JC. Peethambaram PP. Smithson WA. *et al.* Phase II trial of primary chemotherapy followed by reduced-dose radiation for CNS germ cell tumor. *J Clin Oncol* 1999;17:933–940.
15. Kitamura K. Shirato H. Sawamura Y. *et al.* Preirradiation evaluation and technical assessment of involved field radiotherapy using computed tomographic (CT) simulation and neoadjuvant chemotherapy for intracranial germinoma. *Int J Radiat Oncol Biol Phys* 1999;43:783–788.
16. Sutton LN. Radcliffe J. Goldwein JW. *et al.* Quality of life of adult survivors of germinomas treated with craniospinal irradiation. *Neurosurgery* 1999;46:1292–1298.

Int. J. Radiation Oncology Biol. Phys., Vol. 60, No. 1, pp. 335–341, 2004

0360-3016/04/$–see front matter

ELSEVIER

doi:10.1016/j.ijrobp.2004.04.028

PHYSICS CONTRIBUTION

FEASIBILITY OF SYNCHRONIZATION OF REAL-TIME TUMOR-TRACKING RADIOTHERAPY AND INTENSITY-MODULATED RADIOTHERAPY FROM VIEWPOINT OF EXCESSIVE DOSE FROM FLUOROSCOPY

HIROKI SHIRATO, M.D., PH.D., MASATAKA OITA, R.T., KATSUHISA FUJITA, R.T., YOSHIHARU WATANABE, R.T., AND KAZUO MIYASAKA, M.D., PH.D.

Department of Radiology, Hokkaido University Hospital, Sapporo, Japan

Purpose: Synchronization of the techniques in real-time tumor-tracking radiotherapy (RTRT) and intensity-modulated RT (IMRT) is expected to be useful for the treatment of tumors in motion. Our goal was to estimate the feasibility of the synchronization from the viewpoint of excessive dose resulting from the use of fluoroscopy.
Methods and Materials: Using an ionization chamber for diagnostic X-rays, we measured the air kerma rate, surface dose with backscatter, and dose distribution in depth in a solid phantom from a fluoroscopic RTRT system. A nominal 50–120 kilovoltage peak (kVp) of X-ray energy and a nominal 1–4 ms of pulse width were used in the measurements.
Results: The mean ± SD air kerma rate from one fluoroscope was 238.8 ± 0.54 mGy/h for a nominal pulse width of 2.0 ms and nominal 100 kVp of X-ray energy at the isocenter of the linear accelerator. The air kerma rate increased steeply with the increase in the X-ray beam energy. The surface dose was 28–980 mGy/h. The absorbed dose at a 5.0-cm depth in the phantom was 37–58% of the peak dose. The estimated skin surface dose from one fluoroscope in RTRT was 29–1182 mGy/h and was strongly dependent on the kilovoltage peak and pulse width of the fluoroscope and slightly dependent on the distance between the skin and isocenter.
Conclusion: The skin surface dose and absorbed depth dose resulting from fluoroscopy during RTRT can be significant if RTRT is synchronized with IMRT using a multileaf collimator. Precise estimation of the absorbed dose from fluoroscopy during RT and approaches to reduce the amount of exposure are mandatory.

Real-time tumor-tracking radiotherapy, Fluoroscopy, Dosimetry.

INTRODUCTION

Fluoroscopic detection of internal fiducial markers for precise setup of patients has been shown to be useful for static radiotherapy (RT) (1–5) and real-time tracking and gated RT (6–10). Prototype real-time tumor-tracking RT (RTRT) uses two sets of fluoroscopy to detect the internal motion of a metallic fiducial marker in or near the target volume (1). Attention to four-dimensional accuracy in space and time is increasing for tumors in motion when the meticulous dose distribution used in particle therapy (11) and intensity-modulated RT (IMRT) (12–17). Synchronization of IMRT and RTRT is expected to increase the therapeutic ratio for tracking moving tumors.

In our previous studies of RTRT without IMRT, the dose rate in the phantom was measured with thermoluminescence and a surface dosimeter (12, 16). The dose rate at 120 kV with a pulse width of 4 ms was 10.8 mGy/min at the entrance. We concluded that the fluoroscopic dose is negligible for patients treated with 60 Gy to the isocenter. However, because the beam-on time will be longer when we combine RTRT with IMRT using a multileaf collimator, integration of IMRT and RTRT could result in an extremely long treatment time. IMRT using a multileaf collimator requires a radiation time four to five times longer than conventional RT. This may result in unacceptable exposure from the fluoroscopy.

Interventional neuroradiology requires fluoroscopic examination for >30 min, on average, and is known to result in a noticeably high skin dose (18). Gkanatsios *et al.* (19) have shown that the median surface dose during a neuroradiologic diagnostic imaging examination is 1.3 Gy, with a maximal surface dose as great as 5.1 Gy.

These results suggest the importance of precise dose measurement in RTRT when the treatment time needs to be longer than previously estimated. We measured the dose resulting from the use of fluoroscopy in the RTRT system.

Reprint requests to: Hiroki Shirato, M.D., Ph.D., Department of Radiology, Hokkaido University School of Medicine, North-15 West-7, Kita-ku, Sapporo 006-8638, Japan. Tel: (+81)11-706-5975; Fax (+81) 11-706-7876; E-mail: hshirato@radi.med.hokudai.ac.jp

Partly supported by a grant-in-aid from the Japanese Ministry of Education, Sports, Culture, and Science.

Received Oct 21, 2003, and in revised form Apr 2, 2004. Accepted for publication Apr 5, 2004.

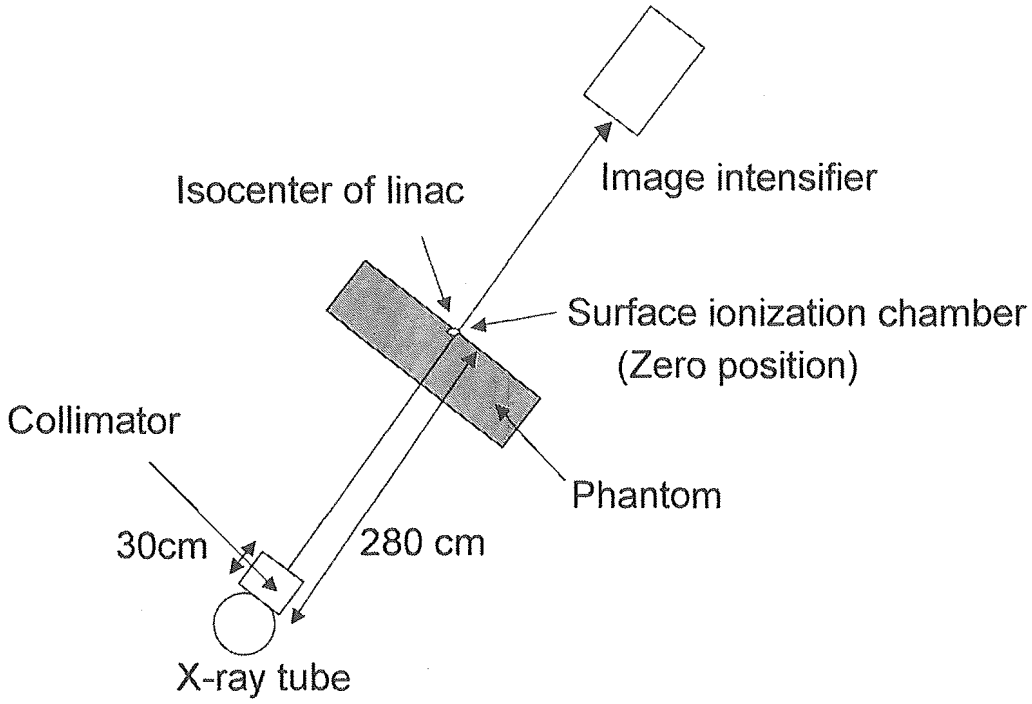

Fig. 1. Geometry of experiments used in this study. Linac = linear accelerator.

METHODS AND MATERIALS

Fluoroscopy

The fluoroscope was a rotating anode X-ray tube assembly (G-1582 BI, Shimadzu, Kyoto, Japan) powered by a three-phase generator. Photons were produced by a 0.6 × 0.6 mm^2 nominal size electron beam incident on a rotating target. We used a pulsed cathode of 80 mA, because it is commonly used clinically. For peak tube potentials of 50–120 kilovoltage peak (kVp), the pulse rate used was a nominal 30 s, with pulse duration of 1.2, 1.6, 2.0, 2.5, and 3.2 ms. The power of the X-ray tube was 1500 kJ for a 0.6-mm focus and 1060 kJ for a 1.0-mm focus. The inherent X-ray filtration was 1.5 mm aluminum equivalent.

The geometries of the fluoroscopy and measurement are shown in Fig. 1. The X-ray beam was collimated to visualize the image of the fiducial markers, which should be placed close to the isocenter. The distance from the X-ray tube to the image detector was 460 cm to avoid collision between the image detectors and the gantry of the linear accelerator. The distance from the X-ray tube (target) to the isocenter of the linear accelerator was 280 cm. The fluoroscopic beam was collimated to 1.6 × 1.9 cm at a 30-cm distance from the tube. The beam size enlarged to 14.5 × 18.5 cm^2 at the isocenter of the linear accelerator where the measurement was performed.

Measurement

The fluoroscopy irradiated field was measured in air using film at the plane including the isocenter perpendicular to the beam axis of the diagnostic X-ray.

The air kerma was measured with a cylindrical chamber with a collecting volume of 3 cm^3, using a Scanditronix WELLHOFER DC300 TNC/160 and a RAMTEC 1500B (Toyo Medic, Tokyo, Japan) designed for diagnostic radiography and mammography. The nominal X-ray energy available for measurement was quoted as 20–150 kV. The wall of the chamber was made of Shonka C552 (1.7 g/cm^3) with the thickness at 0.3 mm. The chamber has an outer length of 41.5 mm and an outer diameter of 10.6 mm. The nominal calibration factor was 9.3 mGy/nC.

The half value layer was measured using varying thicknesses (0.25, 1.05, and 2.05 mm) of a 20.0 × 30.0-cm aluminum (Al) sheet (99.999% Al). The half value layer was measured using a source-to-aluminum filtration distance of 25 cm and a source-to-detector distance of 280 cm.

The dose in air at the isocenter was measured to estimate the air kerma, which does not take into account any backscatter. The distance from the X-ray source to the central axis of the chamber was 280 cm, and the field size was 10 × 14 cm^2. The chamber was positioned on the central axis of the beam, with its long axes parallel to the cathode–anode direction of the X-ray tube.

The percent depth dose (PDD) was measured with a smaller chamber, a farmer-type chamber No. 2591 with a collecting volume of 0.6 cm^3 without a build-up cap in the Solid Water phantom. The ionization chamber was placed on the surface of the phantom, which consisted of 30 × 30-cm^2 slabs of Solid Water, with a total thickness of 10 cm (Fig. 1). The source-to-surface distance was set at 280 cm from the tube. The dose rate at 0.0, 1.0, 2.0, 3.0, 4.0, 5.0, 6.0, 8.0, 10, 12, 15, and 20 cm was measured by changing the depth of the chamber perpendicular to the beam axis for

Table 1. Measured air kerma rate from one fluoroscope at isocenter of linear accelerator according to nominal kVp

	Nominal kVp			
Air kerma rate	50	70	100	120
Mean (mGy/h)	33.50	90.25	238.80	366.18
SD (mGy/h)	0.30	0.15	0.54	0.86
%SD	0.9	0.2	0.2	0.2

Abbreviation: kVp = kilovoltage peak.

a nominal 50-, 70-, 100-, and 120-kVp X-ray beam, respectively. The depth of the camber was adjusted by adding the corresponding 30 × 30-cm^2 slabs of Solid Water, with a total thickness of 1.0–20 cm on the surface of the phantom. The position of the chamber was adjusted to be on the central X-ray beam axis and parallel to the cathode–anode direction of the X-ray tube by visualizing the chamber under fluoroscopy. Correction was made for recombination, polarity, or energy dependence effects. The "surface" measurement at depth 0 was acquired with the center of the cylindrical chamber put at the same plane as the surface of the Solid Water phantom by cutting the surface of the phantom to fit it in. The PDD was normalized at the depth of the maximal dose for each X-ray beam.

The mean ± standard deviation were calculated for each data item on the basis of 10 measurements for each data point.

RESULTS

The half-value layer for each nominal kilovoltage peak of the X-ray tube was estimated to be 2.73, 3.71, 5.02, and 6.72 mm Al for a nominal 50, 70, 100, and 120-kVp X-ray beam, respectively.

The air kerma rate from one fluoroscope was 20.3 ± 0.2, 26.3 ± 0.4, 33.5 ± 0.3, 47.9 ± 0.2, and 68.2 ± 0.3 mGy/h at a nominal pulse width of 1.2, 1.6, 2.0, 2.8, and 4.0 ms, respectively, with a nominal 50-kVp X-ray beam. The air kerma rate from simultaneous exposure of two fluoroscopes with a nominal 50-kVp X-ray beam for 1.6 and 2.0 ms was 58.7 ± 0.5 and 72.7 ± 0.3 Gy/h respectively, which was roughly twice (2.2 times the rate with one fluoroscope) the corresponding dose rate of one fluoroscope.

The air kerma rate measured for one X-ray tube at the isocenter of the linear accelerator is shown in Table 1 for each nominal kilovoltage peak of the X-ray tube using 2.0 ms as the pulse width. The air kerma rate from one fluoroscope was 238.8 ± 0.54 mGy/h for a nominal pulse width of 2.0 ms with a nominal 100-kVp X-ray beam. The relationship between the nominal kilovoltage peak and the air kerma rate is shown in Fig. 2. The air kerma rate increased steeply with the increase in the X-ray beam energy.

The relationship between the pulse width and the surface dose rate, including backscatter, is shown in Fig. 3 according to the nominal kilovoltage peak. The surface dose was 28–980 mGy/h (Table 2). The surface dose was strongly dependent on the kilovoltage peak and linearly increased with the pulse width of the fluoroscope.

The PDD curves for each nominal kilovoltage peak of the X-ray beam are shown in Fig. 4. The dose at 5.0 cm was 37–58% for 50–120 kVp, respectively.

When we put a patient on the treatment couch, the patient's skin surface will receive a greater dose than the dose estimated at the isocenter because of the shorter distance from the X-ray source to the skin surface. Assuming that the distance between the skin entrance and the isocenter, *r*, is

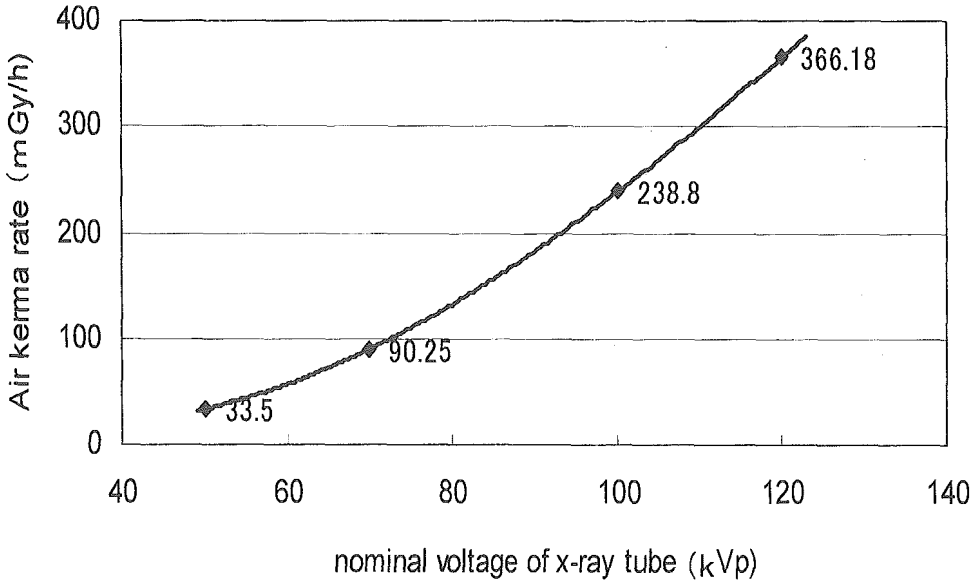

Fig. 2. Relationship between nominal kilovoltage peak of fluoroscopic X-ray and air kerma rate from one fluoroscope.

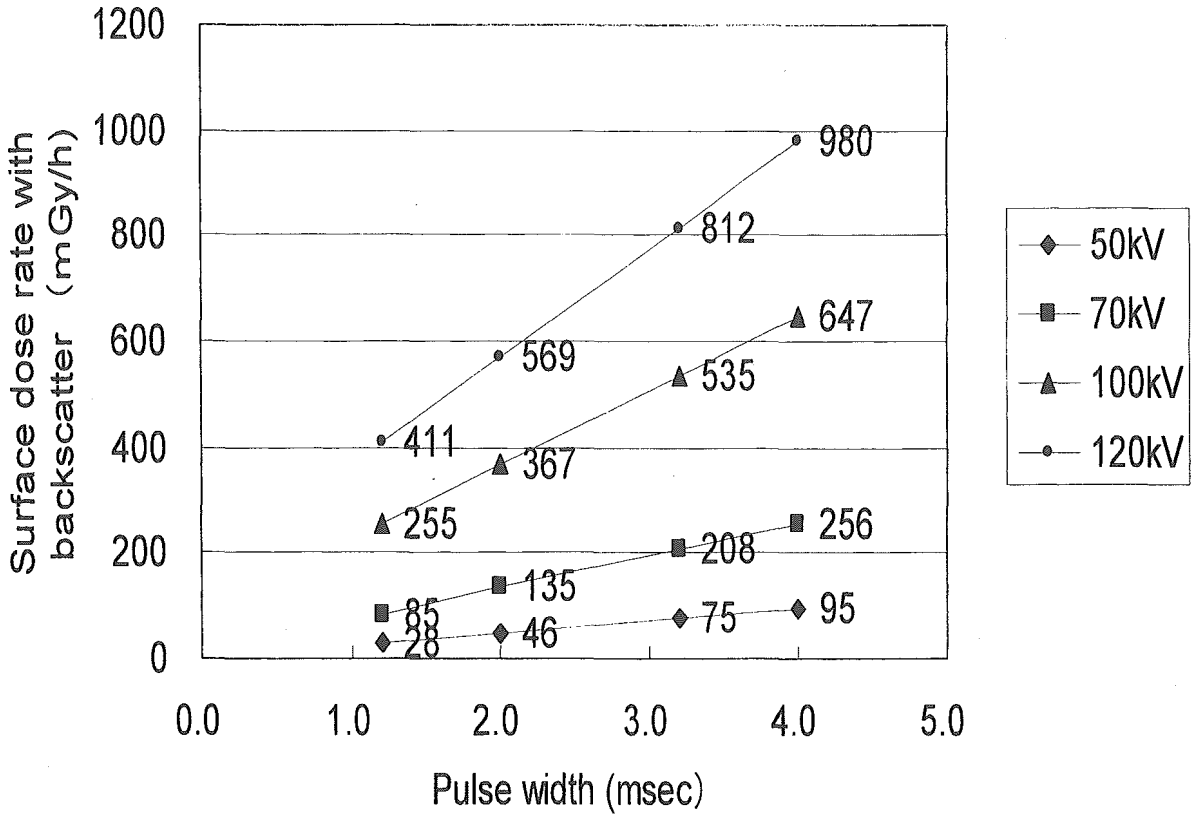

Fig. 3. Relationship between pulse width and surface dose rate from one fluoroscope according to kilovoltage peak. Diamonds, 50 kV; squares; 70 kV, triangles; 100 kV; circles, 120 kV.

5–25 cm, the estimated dose at the skin surface with backscatter (Fig. 5) will be from $r = 5$ cm to $r = 25$ cm. The dose was calculated simply using the formula $R^2/(Rr)^2$, where R is the distance from the X-ray source to the isocenter (280 cm in the RTRT system). The estimated skin surface dose from one fluoroscope in RTRT was 29–1182 mGy/h. The estimated skin surface dose was strongly dependent on the kilovoltage peak and the pulse width of the fluoroscope and slightly dependent on the distance between the skin and isocenter.

DISCUSSION

The Joint Working Party of the British Institute of Radiology and the Hospital Physicists' Association published PDD curves of similar beams measured for use in RT (20). Jennings and Harrison (21) and Harrison (22) have also published the depth dose of diagnostic radiography. Fetterly *et al.* (23) published the X-ray dose distribution of fluoroscopy beams in 2001. These data were based on the measurements using source-to-surface distances of 30–50 cm, far shorter than the source-to-surface distance of 280 cm used in the RTRT system. The greater percentage of dose at each depth in our study compared with those in previous reports for kilovoltage of X-rays may be a result of the longer source-to-surface distance in the RTRT system. We were not able to measure the "surface dose" by parallel chamber with sufficient sensitivity and used a 0.6-cm^3 cylindrical chamber, which could also have been a source of bias in our study. More work is required for precise measurement.

Table 2. Estimated dose rate at skin surface for different pulse widths and kVp values

Pulse width (ms)	Estimated dose rate (mGy/h)			
	50 kVp	70 kVp	100 kVp	120 kVp
1.2	28.4	483.2	255.2	411
2.0	45.9	762.2	366.8	568.5
3.2	75.4	1174.4	535	811.7
4.0	94.7	1448.7	647.4	980.1

Abbreviation: kVp = kilovoltage peak.

The real-time tumor-tracking system has been used with precise setup and gated RT in >200 patients with various tumors, including head-and-neck tumors and tumors of the lung, esophagus, liver, pancreas, prostate, and uterus (1). In this study, we investigated the parameters used in actual RTRT for various tumors. A nominal X-ray strength of 80 kVp and pulse width of 2–4 ms are frequently used for the head-and-neck region, and a strength of 100–120 kVp and duration of 2 ms are used for lung and liver treatment in clinical practice. If the patient's body is large or thick, the system requires 4 ms for visualization of the internal marker.

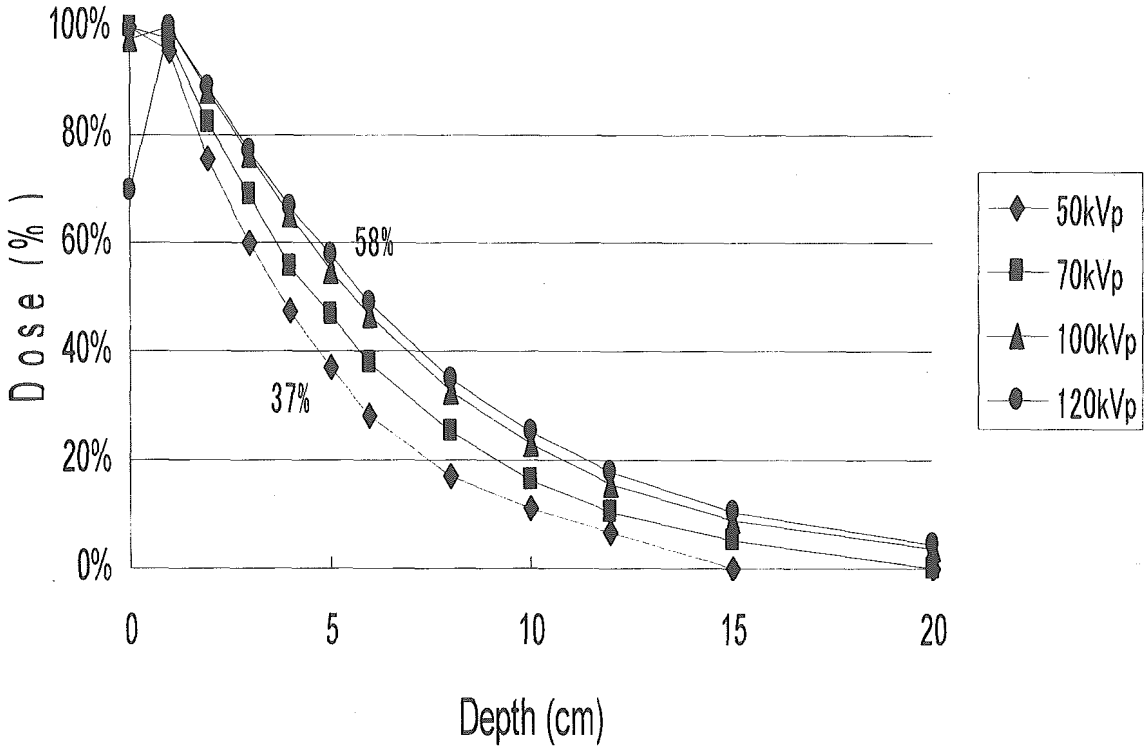

Fig. 4. Percent depth dose curves according to kilovoltage peak of fluoroscope. Diamonds, 50 kV; squares; 70 kV, triangles; 100 kV; circles, 120 kV.

Because RTRT usually requires two sets of fluoroscopy, the maximal dose possible to deliver to the skin surface is two times the dose at the skin surface from one fluoroscope. Usually, the two diagnostic beams do not overlap at the skin surface. However, they could overlap if treating a tumor very close to the skin surface. With the expected RT times needed for IMRT plus RTRT and the exposure parameters required for sufficient image quality, the patient exposure could be unacceptable.

A normal (four fields), 2-Gy, static field treatment is

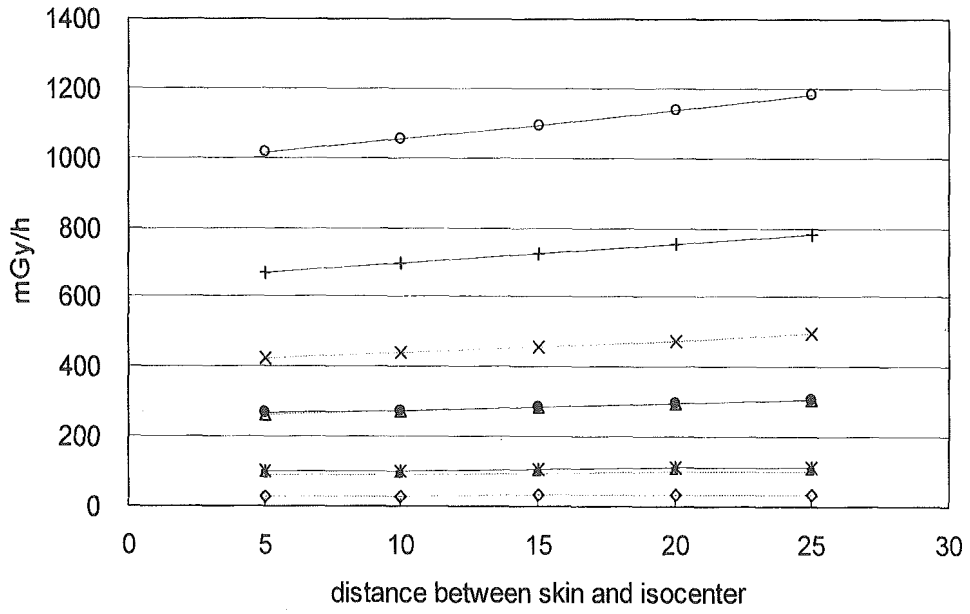

Fig. 5. Relationship between distance from surface to isocenter and surface dose rate from one fluoroscope. Diamonds, 50 kVp, 1.2 ms; asterisks, 50 kVp, 4.0 ms; squares, 70 kVp, 1.2 ms; black circles, 70 kVp, 1.4 ms; triangles, 100 kVp, 1.2 ms; plus signs, 100 kVp, 1.4 ms; crosses, 120 kVP, 1.2 ms; white circles, 120 kVp, 1.4 ms.

≤300 MU approximately. At 300 MU/min and a 25% duty cycle, this would equal 4 min of surveillance time or a skin dose of ~8 cGy (highest case, 120 kVP and 4 ms [Fig. 5], 4 min/60 min × 1.2 Gy/h). If IMRT increases the monitor unit (MU) by a factor of 3–5, the treatment time should be only 12–20 min; however, the fluoroscopic dose becomes worrisome, not so much at the skin but at depth, for which the PDD may not be insignificant. In practice, we have noted that intrafractional fluctuation of tumor motion is often so large that the table position must be adjusted several times by additional fluoroscopic examination (8). In that case, the fluoroscopic dose could extend to 30 min.

In interventional neuroradiology, advances in insertion techniques and catheter materials have increased the acceptable exposure time of diagnostic radiography. The unexpectedly high doses used in modern interventional radiology have raised concerns about radiation safety and protection (18). The results of the present study have confirmed that it is also important to reduce the radiation dose from fluoroscopic exposure during RT. A reduction of the field size is important, but not the perfect answer, because the same area of skin will receive the same dose every day during RTRT. Sharp *et al.* (24) have found that various prediction models, such as a linear model or neural network model, can help reduce the pulse rate to <30 Hz. They considered 14 lung tumor cases in which the peak-to-peak motion was >8 mm and compared the localization error using linear prediction, neural network prediction, and Kalman filtering against a system that used no prediction. They found that by using prediction, the root mean squared error between the predicted and actual three-dimensional (3D) motion was improved for all latencies and all imaging rates evaluated. A reduction in the source-to-detector distance is also useful to reduce the amount of exposure. The attachment of the X-ray tubes and cameras to the gantry head of the linear accelerator can reduce the source-to-detector distance significantly (17). The amount of reduction in the absorbed dose will be about one-third of that of our system, providing that the same dose is required at the surface of the image intensifier. Amorphous silicon directors may reduce the dose required to obtain an image with the same time resolution; the absorbed dose will be further reduced. Changing the fluoroscopy angle according to changes in the therapeutic beam angle beam may also help to reduce the dose to the same skin surface. The shortcoming of the gantry-mounted imaging units may be their inability to use noncoplanar irradiation techniques and the difficulty in maintaining imaging unit accuracy. Also, the X-ray tubes and image detectors can be an obstacle during non-RTRT. Magnetic detection of the metallic marker in the body can eliminate the requirement for fluoroscopic exposure and is also expected to be an alterative to the fluoroscopic detection of internal fiducial markers (25).

We have adapted several approaches to reduce the amount of exposure from fluoroscopy to synchronize RTRT and IMRT. First, software was designed that allows the use of one instead of two sets of fluoroscopy for tracking after registration between the 3D coordinates and the two-dimensional projected coordinates of the marker on one fluoroscopic image. The shortcoming of this method is that two-dimensional projection does not provide information about the third dimension; thus, we have not yet used the two-dimensional projection method in a clinical situation. Second, the pulse rate is now changeable from 30 Hz to 15, 10, 5, and 2 Hz. If the tumor is moving slowly, the lower pulse rate can be used. Third, a 3D trajectory of the tumor is obtained before actual treatment and is used to select the best position for tracking each day to improve gating efficiency. We plan to include the 3D dose distribution of the fluoroscopic beam in our treatment planning system to combine it with the dose distribution of the therapeutic beams. Details of these developments will be described elsewhere.

CONCLUSION

The absolute dose and depth–dose distribution of fluoroscopy in the RTRT system showed that synchronization of RTRT and IMRT may result in an unacceptably high radiation dose to the skin surface and possibly to the deep tissues. The synchronization of RTRT and IMRT requires improvement to reduce fluoroscopic exposure.

REFERENCES

1. Shirato H, Harada T, Harabayashi T, *et al.* Feasibility of insertion/implantation of 2.0-mm-diameter gold internal fiducial markers for precise setup and real-time tumor tracking in radiotherapy. *Int J Radiat Oncol Biol Phys* 2003;56:240–247.
2. Shimizu S, Shirato H, Kitamura K, *et al.* Use of an implanted marker and real-time tracking of the marker for the positioning of prostate and bladder cancers. *Int J Radiat Oncol Biol Phys* 2000;48:1591–1597.
3. Kitamura K, Shirato H, Shimizu S, *et al.* Registration accuracy and possible migration of internal fiducial gold marker implanted in prostate and liver treated with real-time tumor-tracking radiation therapy (RTRT). *Radiother Oncol* 2002;62:275–281.
4. Kaatee RS, Olofsen MJ, Verstraate MB, *et al.* Detection of organ movement in cervix cancer patients using a fluoroscopic electronic portal imaging device and radiopaque markers. *Int J Radiat Oncol Biol Phys* 2002;54:576–583.
5. Poggi MM, Gant DA, Sewchand W, *et al.* Marker seed migration in prostate localization. *Int J Radiat Oncol Biol Phys* 2003;56:1248–1251.
6. Shimizu S, Shirato H, Ogura S, *et al.* Detection of lung tumor movement in real-time tumor-tracking radiotherapy. *Int J Radiat Oncol Biol Phys* 2001;51:304–310.
7. Kubo HD, Wang L. Introduction of audio gating to further reduce organ motion in breathing synchronized radiotherapy. *Med Phys* 2002;29:345–350.
8. Seppenwoolde Y, Shirato H, Kitamura K, *et al.* Precise and real-time measurement of 3D tumor motion in lung due to breathing and heartbeat, measured during radiotherapy. *Int J Radiat Oncol Biol Phys* 2002;53:822–834.

9. Harada T, Shirato H, Ogura S, *et al.* Real-time tumor-tracking radiation therapy for lung carcinoma by the aid of insertion of a gold marker using bronchofiberscopy. *Cancer* 2002;95:1720–1727.
10. Kitamura K, Shirato H, Seppenwoolde Y, *et al.* Tumor location, cirrhosis, and surgical history contribute to tumor movement in the liver, as measured during stereotactic irradiation using a real-time tumor-tracking radiotherapy system. *Int J Radiat Oncol Biol Phys* 2003;56:221–228.
11. Minohara S, Kanai T, Endo M, *et al.* Respiratory gated irradiation system for heavy-ion radiotherapy. *Int J Radiat Oncol Biol Phys* 2000;47:1097–1103.
12. Shirato H, Shimizu S, Kitamura K, *et al.* Four-dimensional treatment planning and fluoroscopic real-time tumor tracking radiotherapy for moving tumor. *Int J Radiat Oncol Biol Phys* 2000;48:435–442.
13. Vedam SS, Keall PJ, Kini VR, *et al.* Acquiring a four-dimensional computed tomography dataset using an external respiratory signal. *Phys Med Biol* 2003;48:45–62.
14. Ford EC, Mageras GS, Yorke E, *et al.* Respiration-correlated spiral CT: A method of measuring respiratory-induced anatomic motion for radiation treatment planning. *Med Phys* 2003;30:88–97.
15. Brock KK, Hollister SJ, Dawson LA, *et al.* Technical note: Creating a four-dimensional model of the liver using finite element analysis. *Med Phys* 2002;29:1403–1405.
16. Shirato H, Shimizu S, Kunieda T, *et al.* Physical aspects of a real-time tumor-tracking system for gated radiotherapy. *Int J Radiat Oncol Biol Phys* 2000;48:1187–1195.
17. Neicu T, Shirato H, Seppenwoolde Y, *et al.* Synchronized moving aperture radiation therapy (SMART): Average tumour trajectory for lung patients. *Phys Med Biol* 2003;48:587–598.
18. Kemerink GJ, Frantzen MJ, Oei K, *et al.* Patient and occupational dose in neurointerventional procedures. *Neuroradiology* 2002;44:522–528.
19. Gkanatsios NA, Huda W, Peters KR. Adult patient doses in interventional neuroradiology. *Med Phys* 2002;29:717–723.
20. Joint Working Party of the British Institute of Radiology and the Hospital Physicists' Association. Central axis depth dose data for use in radiotherapy. *Br J Radiol* 1996;(Suppl. 25).
21. Jennings WA, Harrison RM. X-rays: Half-value thickness range 0.01–8.0 mm Al. *Br J Radiol* 1983;17:1–7.
22. Harrison RM. Central-axis depth-dose data for diagnostic radiology. *Phys Med Biol* 1981;26:657–670.
23. Fetterly KA, Gerbi BJ, Alaei P, *et al.* Measurement of the dose deposition characteristics of x-ray fluoroscopy beams in water. *Med Phys* 2001;28:205–209.
24. Sharp G, Jiang SB, Shimizu S, *et al.* Prediction of respiratory tumor motion for real-time image-guided radiotherapy. *Phys Med Biol* 2004;49:425–440.
25. Seiler PG, Blattmann H, Kirsch S, *et al.* A novel tracking technique for the continuous precise measurement of tumour positions in conformal radiotherapy. *Phys Med Biol* 2000;45:N103–N110.

Acta Neurochir (Wien) (2004) 146: 291–298
DOI 10.1007/s00701-003-0208-x

Acta Neurochirurgica
Printed in Austria

Case Report

Stereotactic radiosurgery for nodular dissemination of anaplastic ependymoma

H. Endo, T. Kumabe, H. Jokura, R. Shirane, and **T. Tominaga**

Department of Neurosurgery, Tohoku University Graduate School of Medicine, Sendai, Japan

Published online February 9, 2004

Summary

Dissemination of primary intracranial ependymoma occurs in 10% of all cases and is difficult to treat, so this may be one of the major reasons for the poor prognosis. Two patients with nodular dissemination of anaplastic ependymoma were treated with repeated stereotactic radiosurgery using the gamma knife (GK), resulting in tumour control over 21 months. GK radiosurgery is a safe and effective treatment option for providing good local control in patients with nodular dissemination of ependymoma.

Keywords: Anaplastic ependymoma; dissemination; gamma knife; stereotactic radiosurgery.

Introduction

Intracranial ependymomas are rare neuro-ectodermal tumours arising from the ependymal cells of the ventricular system, and predominantly occur in children and young adults. Intracranial ependymomas constitute approximately 3% of all intracranial neoplasms and about 10% of all childhood brain tumours [6, 11]. Aggressive multimodality management including surgery, radiation therapy, booster irradiation and chemotherapy have extended the survival time, but the overall survival in most series still does not exceed 60% at 5 years [3, 13, 15, 18]. The pattern of recurrence may be local and/or dissemination to remote sites, and the prognosis after recurrence is quite poor. Dissemination occurs in about 10% of cases of primary intracranial ependymoma [2, 16]. The correlation between prognosis and histological grade of the tumour remains controversial [3, 4, 6, 15, 16, 22], but leptomeningeal dissemination occurs more frequently with high-grade ependymoma than with low-grade ependymoma [16]. The mean survival time after dissemination is 6 months [2].

We treated two patients with anaplastic ependymoma, who manifested multiple nodular dissemination in the course of their disease, by stereotactic radiosurgery (SRS) using the gamma knife (GK). The tumours were controlled for 21 months.

Case reports

Case 1

A 14-year-old girl first presented with headache, nausea and vomiting. She was admitted for treatment of a right lateral ventricular tumour in October 1992. Magnetic resonance (MR) imaging revealed a cystic mass with ring enhancement in the right lateral ventricle, involving the cingulate gyrus (Fig. 1). She underwent subtotal removal of the tumour. Histological examination revealed anaplastic ependymoma. She received 60 Gy of local irradiation and chemotherapy using nimustine hydrochloride (ACNU). She made a complete recovery and radiological study showed no residual tumour. ACNU maintenance therapy was given on an outpatient basis for 1.5 years. She led a normal school life after discharge from our hospital. However, MR imaging performed 4 years and 5 months after the initial treatment revealed a nodular enhanced mass at the cingulate gyrus.

She was treated with GK radiosurgery on four occasions, surgery on three occasions and chemotherapy using cisplatin and etoposide for local recurrences (Table 1). During these treatments, multiple intracranial nodular disseminations occurred. She underwent GK radiosurgery on six occasions for these disseminations in various locations (Table 1, Fig. 2). Fourth ventricular dissemination which first occurred 7 years and 10 months after the initial treatment was treated twice by GK radiosurgery. Although the tumour was controlled for 21 months, MR imaging performed 9 years and 7 months after the initial treatment revealed progression of the tumour. Subtotal removal of the fourth ventricular mass was performed, followed by whole brain irradiation (30 Gy). Follow-up MR imaging performed 9 years and 10 months after

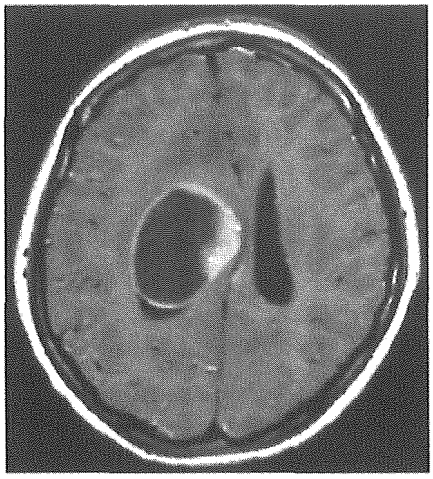

Fig. 1. Case 1: Axial T1-weighted MR image with gadolinium-diethylenetriaminepenta-acetic acid on admission demonstrating a cystic mass with ring enhancement in the right lateral ventricle

the initial treatment showed new dissemination in the anterior horn of the right lateral ventricle, but no enhanced lesion was observed at the primary site and the other nodular disseminations treated by GK radiosurgery were controlled (Fig. 3).

Although the patient developed transient left hemiparesis after the second operation, hemiparesis gradually improved and she began to walk with assistance of mechanical aids. She developed no additional neurological deficits after the third and fourth operations and repeated GK radiosurgery. During these treatments, the patient led a normal school life, entered a nursing school, and passed the national board examination. Her mental status and consciousness was normal, and Karnofsky scale was 70% at the last follow up.

Case 2

A 14-year-old boy presented with headache and nausea persisting for a month. He was admitted for treatment of a fourth ventricular tumour in January 1998. MR imaging revealed a heterogeneous enhanced mass in the fourth ventricle and hydrocephalus (Fig. 4). He underwent subtotal removal of the tumour. Histological examination revealed anaplastic ependymoma. Chemotherapy using cisplatin and etoposide, and local irradiation (33 Gy) by the hyper-fractionated method and craniospinal irradiation (30 Gy) by even-fractionated method were given as adjuvant therapy. Although he suffered from transient lower cranial nerve paresis after the surgery, his neurological condition gradually improved. His first relapse occurred 1 year and 7 months after the initial treatment. MR imaging revealed a small enhanced mass in the fourth ventricle.

GK radiosurgery was performed on three occasions for local recurrence in the fourth ventricle and lower vermis and on three occasions for intracranial nodular dissemination (Table 2, Fig. 5). Multiple nodular disseminations first occurred at 2 years and 4 months after the initial treatment. Nodular dissemination at the thoracic spine occurred 3 years and 10 months after the initial treatment and caused paralysis of the right lower limb and gait disturbance. Surgical removal of the spinal tumour, chemotherapy using ifosfamide, cisplatin and etoposide, and local spinal irradiation (36 Gy) were performed. MR imaging performed 5 months after the surgery showed no residual spinal tumour. MR imaging performed 4 years and 3 months after the initial treatment revealed that the intracranial disseminations were well controlled (Fig. 6). However, follow-up MR imaging performed 4 years and 5 months after the initial treatment revealed diffuse craniospinal dissemination.

During his treatment, the patient led a normal school life and was employed in the computer company after finishing high school. Paraparesis occurred after surgery for the spinal dissemination. His mental status and consciousness was normal, and Karnofsky scale was 60% at the last follow up.

Discussion

The extent of surgical resection is the most consistent factor affecting outcome in cases of intracranial ependymoma [3, 6, 13, 15, 17, 18, 22]. Complete resection can lower the risk of recurrence. The dismal prognosis after recurrence emphasises the importance of the extent of resection at the initial operation. However, complete removal is often not possible and the recurrence rate remains high. The predominant site of relapse is local

Table 1. *Recurrence pattern and treatment for case 1*

Date	Intervals after the initial treatment	Location	Recurrence pattern	Treatment
1992.10.	primary	rt. lateral ventricle of body cingulate gyrus	primary	subtotal removal, LB (60 Gy), ACNU
1997.8.	4 y 5 mo	cingulate gyrus	local 1	GK (25 Gy)
1998.10.	5 y 5 mo	cingulate gyrus	local 2	total removal, CDDP + VP-16
1999.2.	5 y 11 mo	cingulate gyrus	local 3	GK (16 Gy)
1999.10.	6 y 7 mo	cingulate gyrus	local 4	total removal
2000.3.	7 y	cingulate gyrus	local 5	GK (18 Gy)
2001.1.	7 y 10 mo	cingulate gyrus	local 6	GK (22 Gy)
		fourth ventricle	dissemination 1	GK (22 Gy)
2001.2.	7 y 11 mo	cingulate gyrus	local 7	total removal
2001.12.	8 y 9 mo	rt. trigone	dissemination 2	GK (22 Gy)
2002.1.	8 y 10 mo	fourth ventricle	dissemination 3	GK (23 Gy)
2002.5.	9 y 2 mo	septum pellucidum	dissemination 4	GK (23 Gy)
2002.8.	9 y 5 mo	lt. lateral ventricle of body	dissemination 5	GK (23 Gy)
		rt. trigone	dissemination 6	GK (22 Gy)
2002.12.	9 y 9 mo	fourth ventricle	dissemination 7	subtotal removal, WB (30 Gy)

GK Gamma knife radiosurgery; *LB* local brain irradiation; *CDDP* cisplatin; *VP-16* etoposide; *WB* whole brain irradiation.

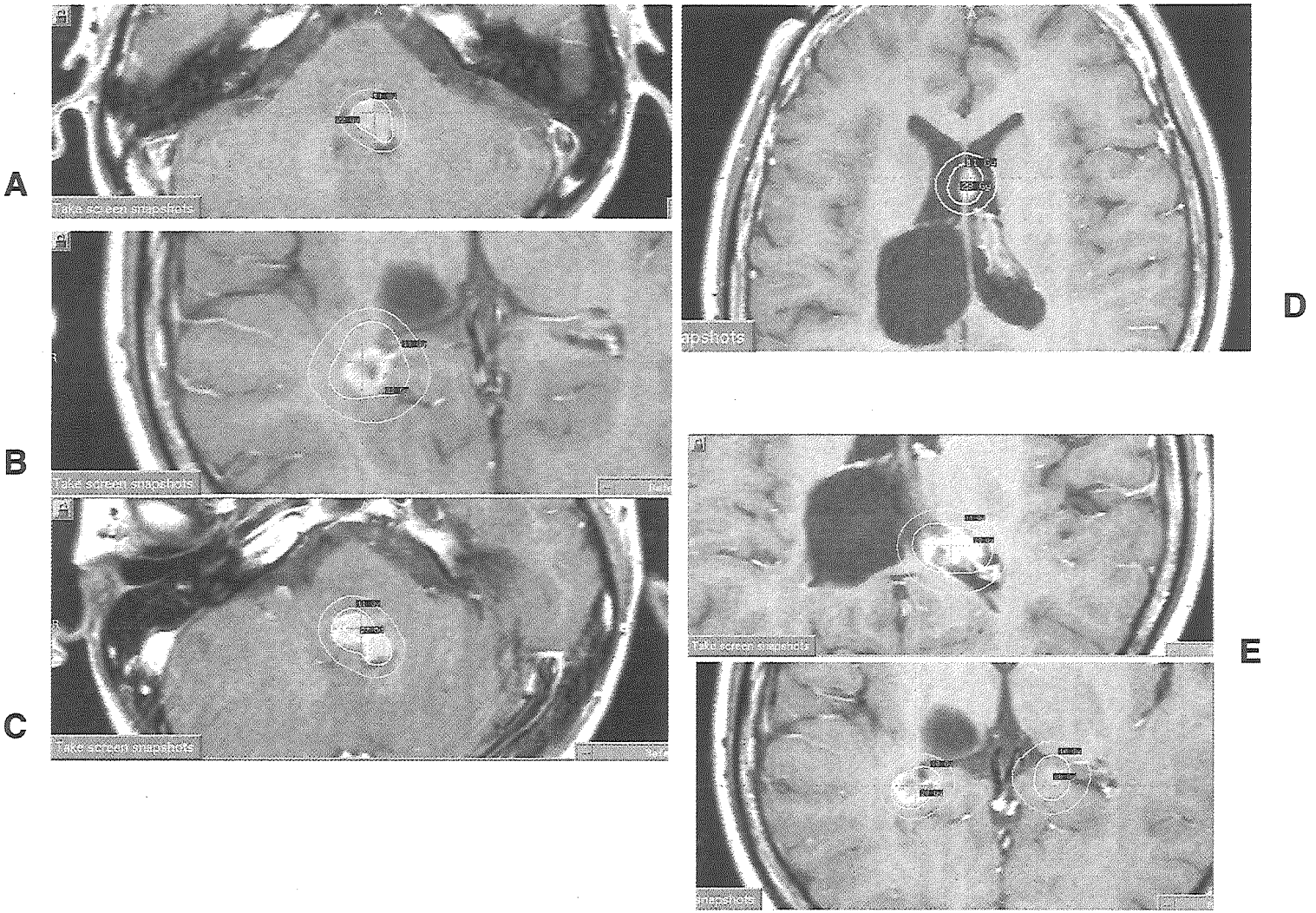

Fig. 2. Case 1: Axial T1-weighted MR images with gadolinium-diethylenetriaminepenta-acetic acid displayed on workstations running the Leksell GammaPlan program. (A) First Gamma knife (*GK*) radiosurgery for fourth ventricular dissemination. (B) First GK radiosurgery for dissemination in the right trigone. (C) Second GK radiosurgery for fourth ventricular dissemination. (D) GK radiosurgery for dissemination in the septum pellucidum. (E) Second GK radiosurgery for dissemination in the right trigone and GK radiosurgery for left lateral ventricular dissemination

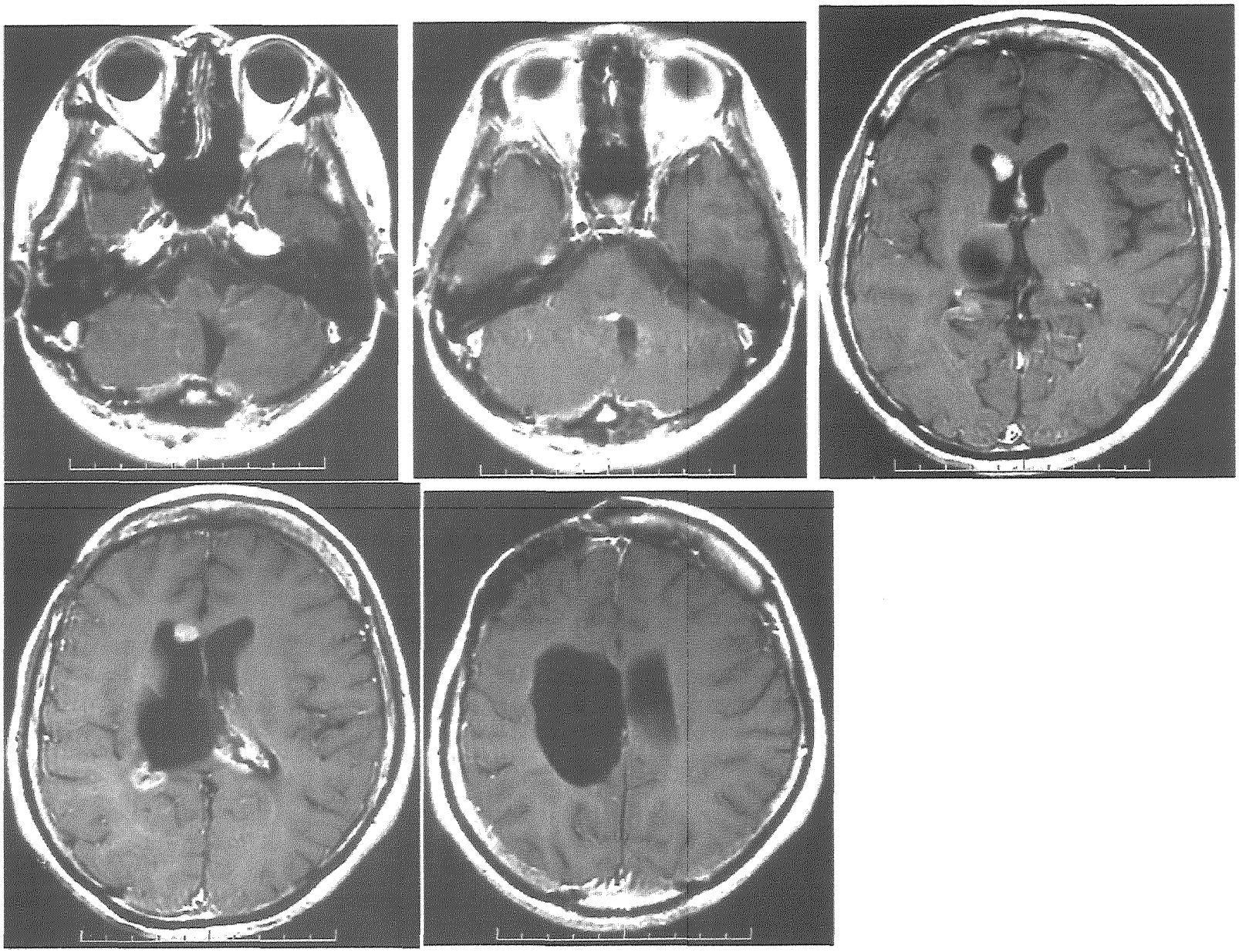

Fig. 3. Case 1: Last follow-up axial T1-weighted MR images with gadolinium-diethylenetriaminepenta-acetic acid performed 9 years and 10 months after the initial treatment showing good control of the primary tumour and multiple nodular disseminations treated by Gamma knife radiosurgery, but new dissemination in the anterior horn of the right lateral ventricle

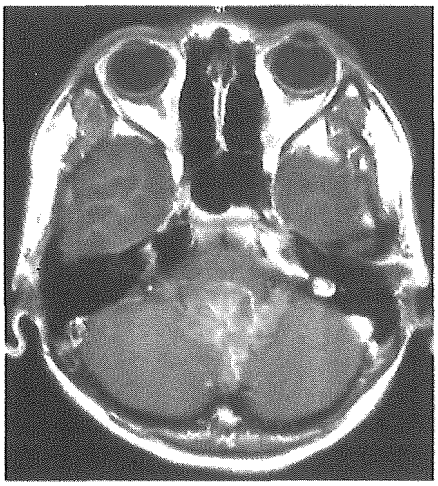

Fig. 4. Case 2: Axial T1-weighted MR image with gadolinium-diethylenetriaminepenta-acetic acid on admission demonstrating a heterogeneous enhanced mass in the fourth ventricle

[19, 20, 23], and postoperative local field irradiation is very suitable for adjuvant therapy [13]. A retrospective study of nondisseminated infratentorial ependymoma suggested that the tumour bed and a safety margin should be the target volume instead of the entire posterior fossa [14].

Dissemination is another important pattern of recurrence in cases of ependymoma. Advances in surgical techniques and adjuvant therapy can control the tumour locally and prolong mean survival time, but the occurrence of dissemination becomes more likely. Dissemination without local recurrence is rare [12]. The incidence of dissemination for primary intracranial ependymoma is about 10% [2, 16]. The high-grade and myxopapillary subtypes are associated with dissemination [16]. Craniospinal irradiation has been advocated for high-grade ependymoma to prevent dissemination [19], but such treatment is not considered as standard.

SRS is effective as a boost after conventional radiation therapy or for the treatment of recurrent disease [1, 5, 7, 8, 10, 21]. Treatment of 22 patients with progressive anaplastic ependymoma using GK radiosurgery as a boost resulted in a median survival time after radiosurgery of 2.2 years and distant recurrence in 9 patients (40.9%) at a mean of 10 months [8]. Treatment of 12 patients with recurrent ependymoma resulted in local control in 68% at 3 years, but two patients suffered distant metastasis, indicating that SRS provided good local tumour control, but dissemination remained an important problem [21].

Treatment of patients with recurrent disseminated ependymomas by SRS has not been reported before. Dissemination may occur in diffuse or loculated patterns [9], and SRS may be indicated for the loculated pattern. The nodular pattern of leptomeningeal dissemination is less common than the diffuse pattern. Medulloblastoma is the most frequent underlying primary tumour to cause nodular dissemination [9]. In our experience, anaplastic ependymomas also tend to cause nodular dissemination, which can be controlled by SRS. Repeated GK radiosurgery controlled nodular disseminated anaplastic ependymoma for 21 months without neurotoxicity in our two patients. Among six previous cases of disseminated ependymoma, one patient received no treatment for dissemination, three were treated with radiation therapy and two were treated with chemotherapy [2]. The mean survival time after the treatment of dissemination was 6 months [2]. Considering that our two patients were still alive at last follow up and the disseminated tumour was controlled for more than 21 months, SRS seems to be effective in the treatment of dissemination. Beyond the first relapse, there is little hope for long-term survival with conventional therapy [4]. Although SRS is not the treatment to cure the disease, it might be the

Table 2. *Recurrence pattern and treatment for case 2*

Date	Intervals after the initial treatment	Location	Recurrence pattern	Treatment
1998.1.	primary	fourth ventricle	primary	subtotal removal, LB (33 Gy), WB & WS (30 Gy), CDDP + VP-16
2000.4.	1 y 8 mo	fourth ventricle	local 1	GK (18 Gy)
2000.11.	2 y 3 mo	vermis	local 2	GK (18 Gy)
2000.12.	2 y 4 mo	corpus callosum	dissemination 1	GK (22 Gy)
2001.8.	3 y	fourth ventricle	local 3	GK (20 Gy)
2001.12.	3 y 4 mo	corpus callosum	dissemination 2	GK (22 Gy)
2002.5.	3 y 9 mo	rt. lateral ventricle of body	dissemination 3	GK (25 Gy)
2002.6.	3 y 10 mo	spinal cord (T7-9)	dissemination 4	subtotal removal, LS (36 Gy), IFOS + CDDP + VP-16

GK Gamma knife radiosurgery; *LB* local brain irradiation; *WB & WS* whole brain & whole spine irradiation; *CDDP* cisplatin; *VP-16* etoposide; *T* thoracic spine; *LS* local spine irradiation; *IFOS* ifosfamide.

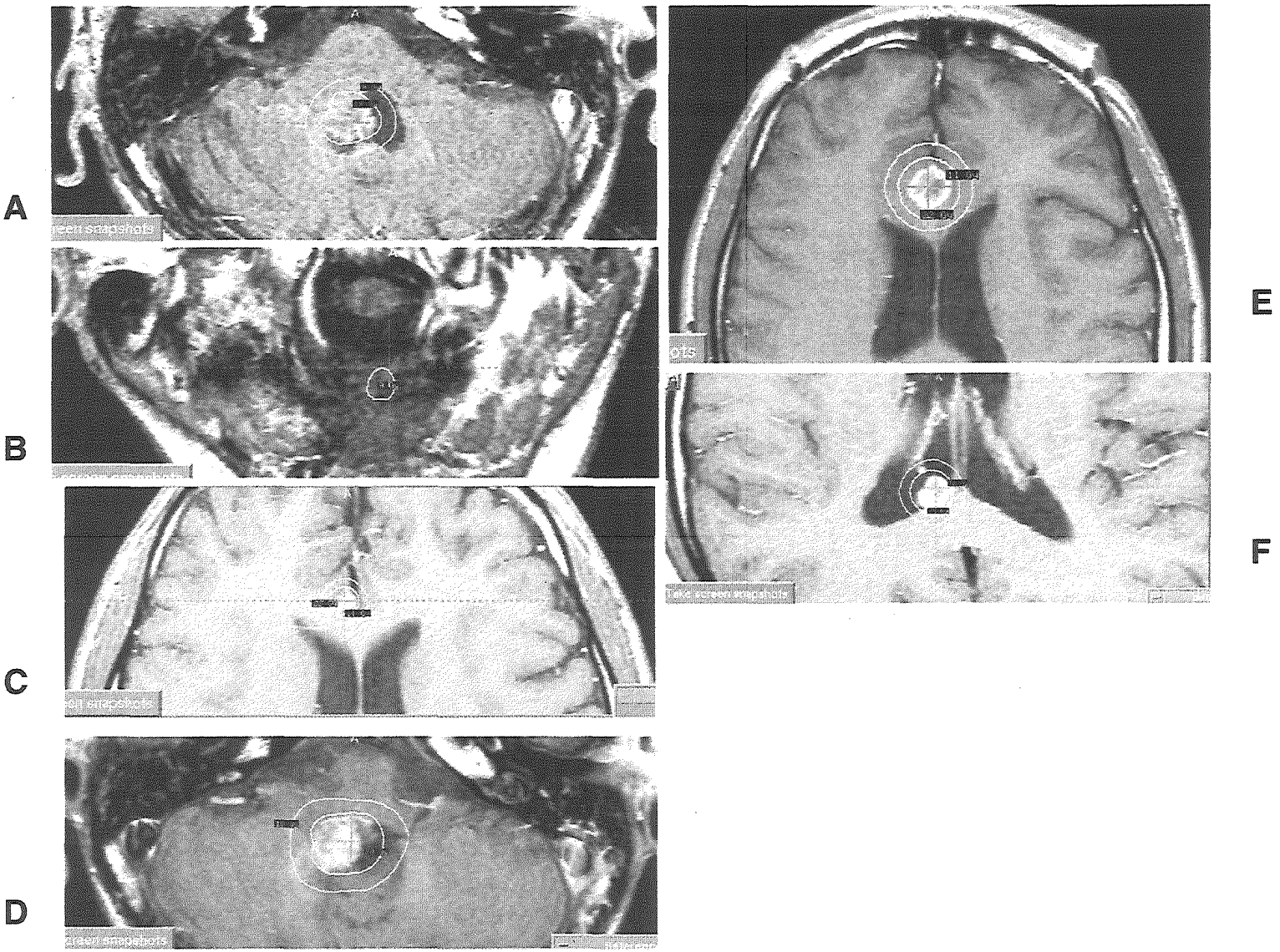

Fig. 5. Case 2: Axial T1-weighted MR images with gadolinium-diethylenetriaminepenta-acetic acid displayed on workstations running the Leksell GammaPlan program. (A) First Gamma knife (*GK*) radiosurgery for local recurrence. (B) Second GK radiosurgery for local recurrence. (C) First GK radiosurgery for dissemination in the corpus callosum. (D) Third GK radiosurgery for local recurrence. (E) Second GK radiosurgery for dissemination in the corpus callosum. (F) GK radiosurgery for dissemination in the right lateral ventricle

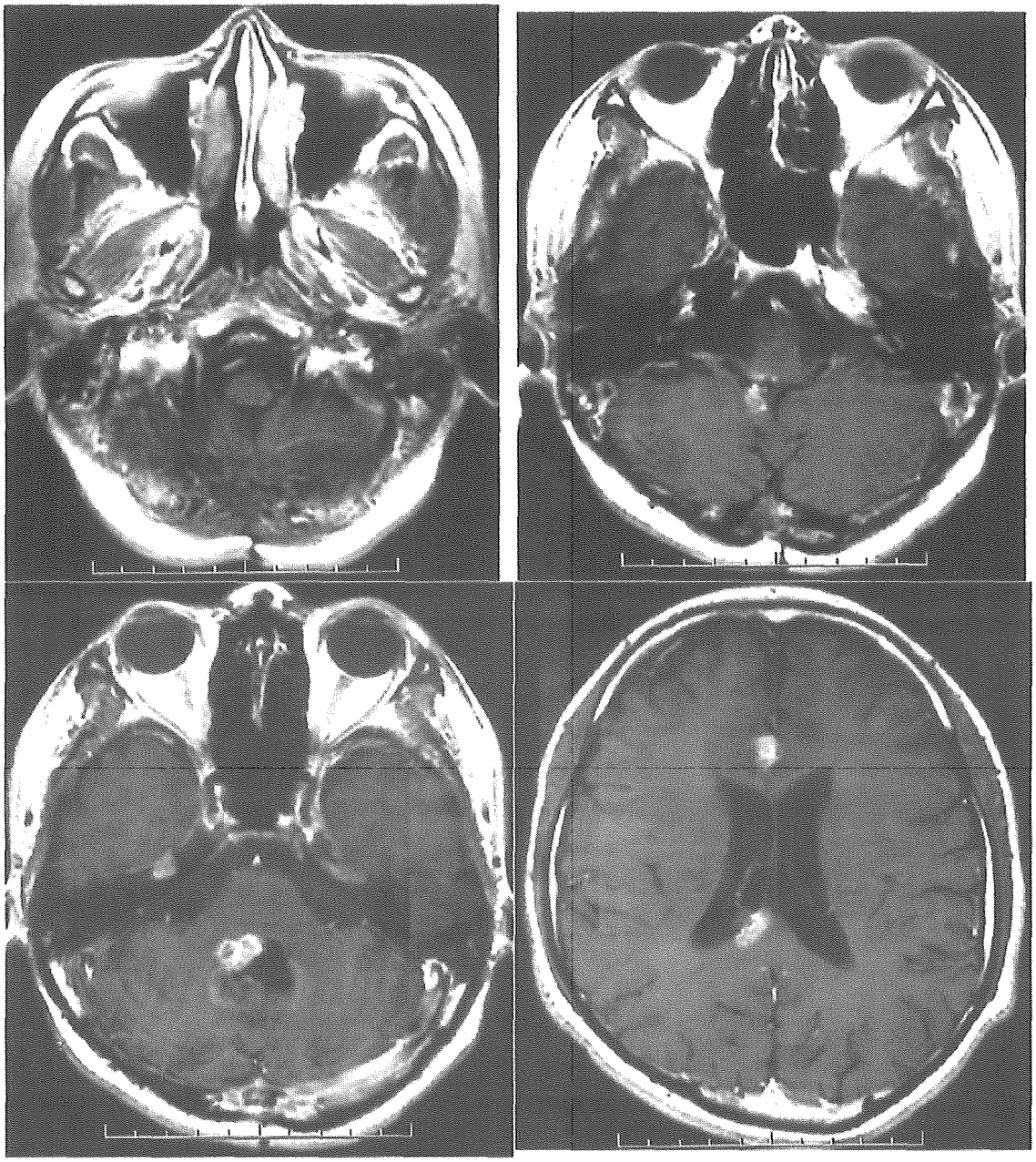

Fig. 6. Case 2: Axial T1-weighted MR images with gadolinium-diethylenetriaminepenta-acetic acid performed 4 years and 3 months after the initial treatment showing nodular enhanced masses in the fourth ventricle, vermis, right lateral ventricle, and corpus callosum

treatment of choice if the patient could benefit from aggressive treatment.

Conclusion

Dissemination is the final form of ependymoma and is difficult to treat. GK radiosurgery can provide safe and effective local control in patients with nodular dissemination of ependymoma. In addition, GK radiosurgery can be repeated because of its minimal neurotoxicity. Although out-of-field tumour progression remains a problem, GK radiosurgery may be the treatment of choice for patients with nodular dissemination.

References

1. Aggarwal R, Yeung D, Kumar P, Muhlbauer M, Kun LE (1997) Efficacy and feasibility of stereotactic radiosurgery in the primary management of unfavorable pediatric ependymoma. Radiother Oncol 43: 269–273
2. Calvo FA, Hornedo J, De La Torre A, Sachetti A, Arellano A, Aramburo P, Aragon G, Otero J (1983) Intracranial tumors with risk